# Conformation-dependent dipoles of liquid crystal molecules and fragments from first principles

C. J. Adam, S. J. Clark, G. J. Ackland, and J. Crain
*Department of Physics and Astronomy, The University of Edinburgh, Edinburgh, EH9 3JZ, Scotland, United Kingdom*
(Received 18 November 1996; revised manuscript received 11 February 1997)

We determine accurate molecular dipole moments for mesogenic fragments and liquid crystal molecules from quantum mechanical computer simulations adapted from large-scale electronic structure calculations on periodic solids. We employ density functional theory and use *ab initio* pseudopotentials for the interaction between valence electrons and ions and the generalized gradient approximation to account for the many-body effects of exchange and correlation. Periodic boundary conditions are enforced so that the molecular electronic wave function can be expanded in terms of a plane wave basis set. We test our method on several small molecules and then apply it to determine the direction, position and dipole moment magnitude for 4-4' pentyl-cyanobiphenyl (5CB) (and related fragments), phenyl benzoate, and 2-2'difluorobiphenyl. For the latter compound, we parametrize a torsional potential for rotation about the dihedral bond. We perform full structural optimization, and find that the torsional barrier heights for fully relaxed molecular structures are substantially reduced relative to nonoptimized geometries. We then demonstrate the influence of conformation and temperature on the molecular dipole moment. We also find that simple vector addition of dipole moments of fragments provides a good estimate of the total dipole moment of the complete molecule. We compare our results to experiment and to conventional quantum chemistry methods where data is available.
[S1063-651X(97)13705-9]

PACS number(s): 61.30.Cz, 42.70.Df, 33.15.Bh, 31.15.Ew

## I. INTRODUCTION

The spontaneous molecular ordering which is characteristic of liquid crystalline phases, has long been exploited in many technological applications such as electro-optic display devices [1–3]. The efficiency of these devices depends on the realignment of the director by an applied electric field through a process which involves interaction between the field and the dielectric torque. The strength of this interaction is related to the sign and magnitude of the anisotropy, $\Delta\epsilon$, of the dielectric constant which couples the external electric field to the liquid crystal medium. The dielectric anisotropy may be positive or negative, depending upon the detailed chemical structure of the constituent molecules, and has a significant dependence on the magnitude and direction of the dipole moment [2]. Polar liquid crystals with strong positive dielectric anisotropies tend to operate at lower voltages and require less power. These polar mesogens also exhibit a much richer phase diagram than do conventional liquid crystals [4]. Electrostatic properties are also influential factors in bulk phase stability, particularly in determining the location and breadth of smectic phases [5]. Classical molecular dynamics simulations have shown that addition of simple models of the dipolar interactions can have significant effects, possibly accounting for up to 30% of the free energy [6]. Although the inclusion of dipolar interactions is computationally costly, it is of importance, hence recent Monte Carlo simulations have been aimed at understanding the influence of the magnitude and direction of molecular dipoles on mesophase formation [7].

Typically, the most reliable experimental method currently used to measure the molecular dipole moment involves separating out the orientation polarization and the distortion polarization from the total polarization [8]. This can be done by measuring the total molar polarization over a range of temperatures in a nonpolar solution, and applying the Debye and Clausius-Mosotti equations [9]. This method, however, has drawbacks in that it is not possible to find the absolute direction of the dipole relative to the molecular axes, and it is difficult to estimate the influence of the solvent on the final results [10].

In view of these practical difficulties and the increasing urge to to predict the properties of as yet unsynthesised molecular materials, it is evidently of considerable importance to develop computational methods for the calculation of properties such as the dipole moment. The problem is not straightforward: It involves not only an accurate method of obtaining the dipole moment from a given electronic configuration and molecular shape, but also a means of determining the probability of conformers which is used as a statistical weighting for the molecular dipole. Presently, unfavorable system size scaling has precluded the application of conventional computational methods to the large molecules that form mesophases [11].

This has also led to a relatively poor understanding of the relationship between the microscopic properties of individual molecules and the observable macroscopic properties of the bulk material. It is well known, for example, that subtle alterations in molecular structure can have profound effects on the stability and properties of mesophases [12]. The ability to engineer molecules that have the desired bulk properties is the ultimate goal of many research studies into liquid crystals and other molecular electronic materials. To achieve this goal, a deeper understanding of molecular properties is essential in providing a basis for detailed exploration of structure-property relationships.

It was very recently demonstrated that techniques for large scale first-principles electronic structure calculations on periodic solids can be adapted successfully to handle isolated molecules [11]. So far, the technique has been applied to

 

determine the equilibrium geometry, vibrational frequencies, and conformational energy landscapes of 4-4' pentylcyanobiphenyl 5CB and cyanobiphenyl 0CB [11, 13]. Comparisons with experimental results, where available, have been good. In this paper, we extend the method to extract conformation-dependent molecular dipoles for a variety of liquid crystals and mesogenic fragments which contain atoms of widely differing electronegativity. In general, we expect the molecular dipole to be defined either by a fixed molecular bond or by the relative position of the most electronegative species. In the former case we expect a weak dependence of the molecular dipole on conformation, while a more pronounced effect is expected in the latter situation.

As examples of these cases we examine phenyl benzoate (which has a highly polar C=O bond) and therefore falls into the former category. The mesogenic fragment 2-2'difluorobiphenyl is in the second category, where the relative positions of the fluorine atoms depend on the dihedral angle between the phenyl groups. Therefore the molecular dipole is expected to have a strong conformation dependence. For both of these materials we quantify the effects that the structure and conformational changes have on the dipole. We also consider the prototype nematogen 5CB, for which the dominant contribution to the molecular dipole is expected to arise from the highly polar CN group, but for which the quantitative effects on the molecular dipole of the alkyl chain and the phenyl rings are uncertain. Therefore we assess the degree to which the total molecular dipole can be estimated from the individual moments of the mesogen fragments, and therefore gain insight into the influence of charge transfer.

The paper is organized as follows. In Sec. II we outline the basic theory and computational implementation of our method, with particular emphasis on solving for the molecular electronic structure, the analogy with periodic solids, and the method of extracting the molecular dipole. We then proceed to discuss the results of test calculations before proceeding to our findings on fragments and mesogens.

## II. METHOD

### A. Molecular electronic structure

#### *1. Theory and algorithms*

We apply density functional theory using the Cambridge-Edinburgh Total Energy Package (CETEP code) [14,15]. We use *ab initio* pseudopotentials (in Kleinman-Bylander form) [16] and the generalized gradient approximation [17], to the exchange and correlation energy, to solve for the electronic ground state of the molecule. The details of this method, as applied to infinitely extended crystals, can be found in [18,19]. In this section we will give only those details which are relevant to the molecular case. The *ab initio* pseudopotentials used for the constituent atoms in the molecules under investigation in this paper are determined according to the scheme of Lin *et al.* [20]. The generalized gradient approximation deals with many-body effects, and is an extension of the local density approximation. It states that the exchange and correlation energy of an electron distribution at a given density and density gradient can be treated as being equivalent to that of an electron gas at that density and density gradient.

We isolate the molecule in a periodically repeated supercell which enforces periodic boundary conditions and allows for the wave functions to take on the form of infinitely extended, delocalized Bloch functions. Specifically, the wave functions of a given electron are of the form

$$\psi(\vec{r}) = \Omega^{-1/2} \sum_j C_j e^{i(\vec{k}+\vec{G}_j)\cdot\vec{r}}, \tag{1}$$

where $\Omega$ is the system volume. The vector $\vec{G}$ is (by analogy with the electronic structure of perfect crystals) a reciprocal lattice vector. Each individual molecular valence electron wave function is expanded in this plane wave basis set up to a cutoff energy. $C_i$ are therefore the expansion coefficients. According to this formalism, the molecular electronic wave function is described by a Fourier series rather than the usual quantum chemistry basis sets.

The introduction of artificial periodicity into the description of the molecular electron wave function allows the problem to be handled exactly as in the case of a perfect crystalline solid. In the limit of large separation between the lattice points of this periodic system, the properties of the isolated molecule are obtained accurately. This is discussed in more detail below.

In the present work only a single $k$ point (Brillouin zone center, by analogy with crystalline band structure terminology) is required as the sampling point ($\vec{k}=0$). Finer sampling is not necessary, since electronic bands are dispersionless for isolated molecules. The size of the basis set (number of plane waves) required to span the molecular wave function is determined by the depth of the ionic pseudopotentials which are used to represent the electron-ion interactions.

This approach has many advantages over conventional localized basis set methods. The set of plane waves is complete and orthonormal, it can be indexed by a single vector quantity and requires no *a priori* knowledge of the electronic distribution. The wave vectors associated with plane waves run from zero up to some specified value given by a plane wave cutoff. Calculating the total energy convergence with respect to basis set size gives an easily defined check on convergence with respect to basis set size.

The coefficients of the plane waves in the expansion are then used as variational parameters until the lowest energy electronic configuration is found for a given set of ion positions. We employ preconditioned conjugate gradients as the minimization algorithm, as this has been found to lead to fast convergence [18]. In all cases, the minimization is subject to the constraint that the electron wave functions be kept orthogonal to each other. The minimization problem is distributed on 256 nodes of a Cray T3D.

#### *2. Details for specific molecular systems*

The molecular valence electron wave functions for all the molecules (except those including fluorine atoms), were expanded in a plane wave basis set with a cutoff energy of 700 eV. A larger basis set is required to represent the highly oscillating states arising from the deeper pseudopotential of fluorine, necessitating a cutoff of 1000 eV [20]. For hydrogen (as it only has a single electron) a pure Coulomb poten-

tial is used. The electronic degrees of freedom were relaxed until the total energy of the molecule was converged to within $10^{-6}$ eV/molecule.

### B. Optimization of atom positions

The structure of a given molecule is determined by a set of bond lengths, bond angles, and torsional angles. A given conformation corresponds to a fixed torsional angle at which all other degrees of freedom can be relaxed. A plausible initial molecular geometry is chosen for an isolated molecule. Geometries for the large molecules were taken from a molecular modeling package [21], without any form of optimization from that package. We then optimize the geometry under given constraints as follows: the Hellmann-Feynman force on each atom in the molecule is calculated, and the atoms are moved under the influence of these forces until no force component exceeds some tolerance. Structure optimization is converged when residual forces on the atoms are below 0.1 eV/Å. For these calculations, molecular point group symmetry is not enforced, since we also wish to examine small symmetry breakings that may occur. In our calculations, finite temperature effects are not included. We therefore do not consider consequences such as anharmonic bond lengthening.

### C. Calculation of the molecular dipole moment

Once the relaxed electronic structure for a given molecular conformation has been found, the calculation of the molecular dipole moment can be made. It can be determined by taking the vector difference between the locations of the centroids of both the electronic and ionic charge distributions. The valence charge density is computed on a discrete fast-Fourier-transform (FFT) grid, and it is obtained directly from the wave functions.

The size of the FFT grid depends on supercell size and cutoff energy. As the $\Gamma$ point is used as the only sampling point, we are only concerned with real (as opposed to complex) wave functions, which halves the computational cost of the calculation. As an example, for the calculation on 2-2' difluorobiphenyl the supercell dimensions were $15\times10\times10$ Å, necessitating a FFT grid size of $160\times108\times108$. The charge density of the molecule is then therefore mapped by approximately 2 000 000 points.

As a plane wave basis set requires periodic boundary conditions, we have to ensure that the molecules are isolated from their periodic image, as described above. We can easily calculate the total energy and dipole moment per unit cell (i.e., per molecule) using the standard solid state technique of the Ewald sum. The long range Coulomb interaction energy between supercells sums to zero, since infinite $\mathbf{G}=\mathbf{0}$ terms cancel exactly. Also, the dipole term is weak, and produces a field which decreases into the surrounding vacuum. The effect of ignoring the additional potential arising from this field can be made arbitrarily small by increasing the size of the unit cell. Varying the unit cell size until the total energy is converged is not a strict enough criterion to test the isolation of the molecule; one must also test for the convergence of the dipole moment. An example of this is shown in Figs. 1(a) and 1(b), where the weak dipole-dipole interaction can be made arbitrarily small at large separation, and is overcome by a strong repulsion due to wave function overlap at small separation. We perform all the subsequent simulations where total energy and dipole moment have converged. Molecules are isolated such that the smallest separation between atoms in adjacent periodic cells was typically 5–6 Å. Higher order electric multipole moments of the molecule will also be converged by this point, as the electric field falls off as increasingly higher powers with distance.

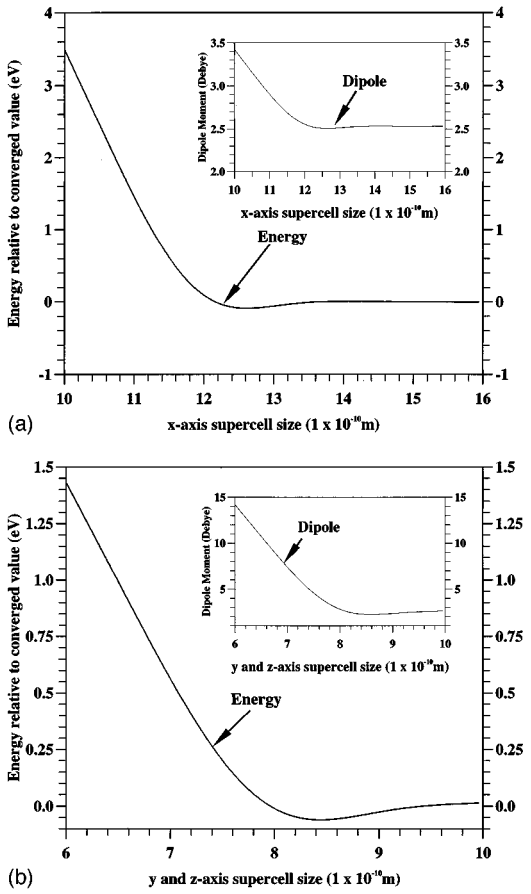


FIG. 1. Curves showing the convergence of the total energy and the dipole moment with increasing supercell size for the molecule 2-2' difluorobiphenyl. The long molecular axis lies along the *x* axis. (a) shows the curve parallel to the molecular axis and (b) gives the curve for the perpindicular directions.

## III. RESULTS AND DISCUSSION

### A. Test calculations: Dipole moments of small molecules

To test the validity of our algorithm, we performed tests on the small molecules $H_2O$, HF, and CH. The results shown in Table I show good agreement with experimental values [22]. Initial starting geometries for $H_2O$ were such that the hydrogen atoms were placed to form a right angle to one another at a distance of 1 Å from the oxygen. For HF and CH the atoms were also placed 1 Å apart. The results of structural optimization for these test molecules are also shown in Table I as are the results of localized basis set DFT calculations for comparison [22]. These results give us confidence to tackle much larger molecules such as 5CB and phenyl benzoate.

A consideration of symmetry shows that a molecule cannot have a dipole moment if it possesses a center of symme-

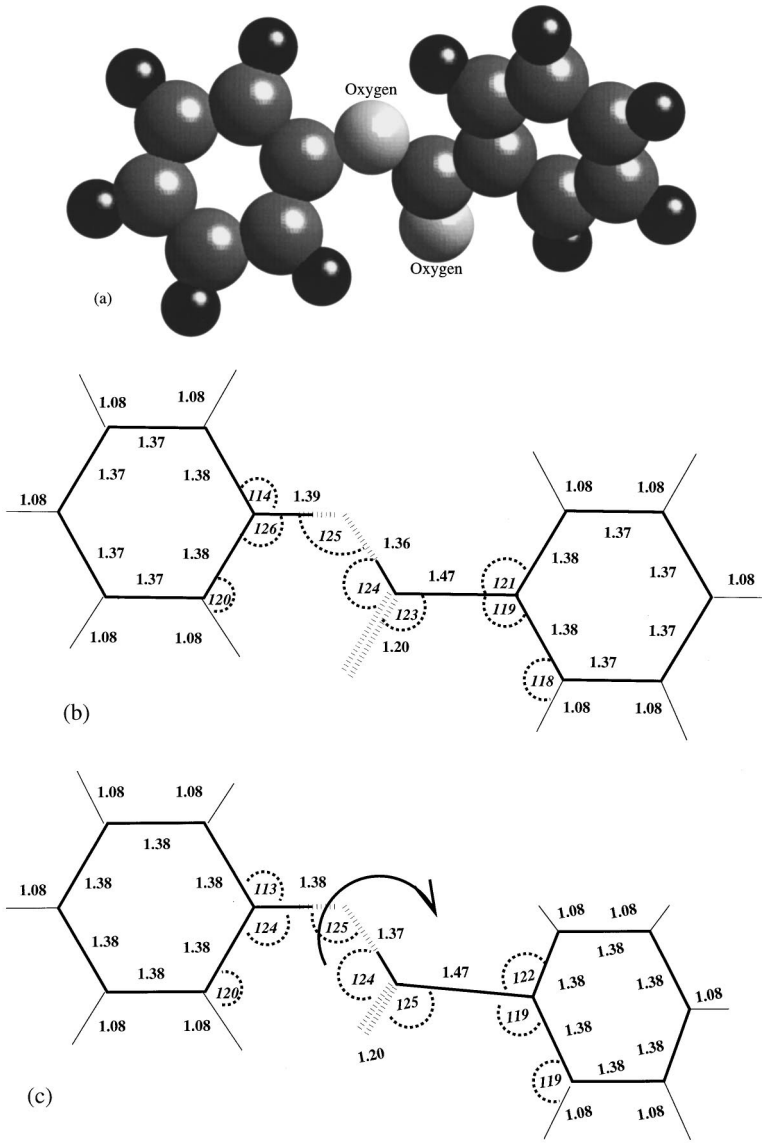


FIG. 2. Illustration of the molecule phenyl benzoate in its 50° conformation (a) and optimized structures for the two conformations investigated: (b) 0° and (c) 50°. The bond lengths are given in Å and the angles in degrees.

try, or if it has symmetry $C_{nh}$ or $D_{nh}$ $(n>1)$ (a rotation axis normal to the mirror plane) or if it has more than one axis of rotational symmetry or an inversion center [10]. We have calculated the dipole moment for the nonpolar molecule methane. To our level of convergence on electronic and molecular structure with no enforced symmetries, we find the dipole to be 0.004 D. We expect this to be the upper level of noise in the subsequent calculations, which is negligible in relation to the magnitudes found for polar mesogenic fragments and molecules.

### B. Electrostatic dipole moments of liquid crystal molecules and fragments

#### *1. Phenyl benzoate*

Phenyl benzoate [an illustration is shown in Fig. 2(a)] with oxygen or sulfur atoms in the ester link and various terminal groups are considered to be promising molecules in liquid crystal synthesis [23]. The dipole moment in the ester function is seen to play an important role in governing the optical anisotropy and phase stability. We have calculated

TABLE I. This table shows our calculated dipole moments and bond distances ($r$) of the small molecules $H_2O$, HF, and CH. Also shown are the experimentally observed values and those calculated using a computational chemistry package [11] incorporating density functional theory (DFT) and a local basis set.

| Molecule (Symmetry) | Dipole ($D$) This work | r (Å) This work | Dipole ($D$) DFT with 6-31G* | r (Å) DFT with 6-31G* | Dipole ($D$) Observed | r (Å) Observed |
|---|---|---|---|---|---|---|
| $H_2O$ ($C_{2v}$) | 1.92 | 0.96 | 2.09 | 0.98 | 1.85 | 0.96 |
| HF ($C_{\infty v}$) | 1.85 | 0.92 | 1.84 | 0.94 | 1.82 | 0.92 |
| CH ($C_{\infty v}$) | 1.54 | 1.21 | 1.31 | 1.14 | 1.46 | 1.20 |

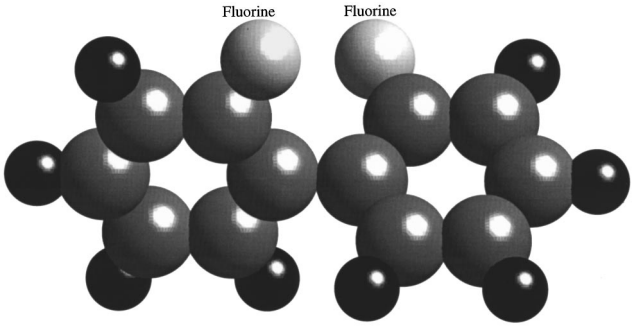


FIG. 3. Illustration of 2-2' difluorobiphenyl in its lowest energy conformation.

the dipole for phenyl benzoate (with oxygen in the ester link) for two conformations around the middle rotator.

The initial geometry was taken from a molecular modeling package without any form of optimization [21]. The bond lengths were set such that the C-C, C-H, and C-O bonds were 1.408, 1.020, and 1.331 Å, respectively. We use a supercell with dimensions $15\times10\times10$ Å and used a plane wave cutoff of 700 eV (25 000 plane waves per electron). Optimized structures were calculated for two conformations; the planar conformation and one with a rotation of 50° around the middle rotator. Recent NMR work shows the planar conformation to be the most stable of the two [24]. Both geometries and schematic representations of the conformations are shown in Figs. 2(b) and 2(c). These conformations were chosen on the basis that the C=O double bond, which is thought to be responsible for the majority of the dipole moment (as the oxygen has a lone pair of electrons), was lying in two easily differentiated planes. Our calculations show this to be the case, as the dipole vector in both conformations is collinear with the C=O bond. However, the magnitude does change, increasing from 2.07 D in the planar conformation to 2.45 D for the 50° rotation. We attribute this to differences in the optimized molecular structures, shown in Figs. 2(b) and 2(c). Although the molecular dipole can mostly be attributed to a specific bond within the molecule, the conformation can change the magnitude by up to 15%. The relative energy differences between the conformations were found to be 0.202 eV/molecule, with the planar conformation the most stable [25].

A recent calculation of the molecular dipole of phenyl benzoate was performed using the HYPERCHEM computational package [26]. The authors calculated the dipole magnitude as 2.65 D and found it to be largely parallel to the C=O double bond but out of plane. No explanation for the dipole being in this position was given, nor was the accuracy of their calculation, and no conformation dependence was considered.

#### *2. 2-2' difluorobiphenyl*

There has been recent interest in understanding the effect that fluorination of the central core has on liquid crystalline characteristics [27,28]. The liquid crystal fragment 2-2' difluorobiphenyl consists of two phenyl groups, with a fluorine atom replacing one of the hydrogens on each group as shown in Fig. 3. We calculated the dipole moment with respect to the conformation and the torsional potential curve for this material. It was expected that the molecular dipole moment will be a sensitive function of the torsional angle, since this governs the relative positions of the fluorine atoms. The geometry for each conformation was optimized to our level of convergence on molecular structure (see above), and the curves relating to these calculations are termed *fully optimized*. We also performed calculations with a fixed geometry at each conformation, in order to quantify the effect full optimization has on the torsional potential and dipole moment. The curves relating to these calculations are termed *nonoptimized*, although the fixed geometry used was an optimized geometry specific to a chosen conformation.

The calculations were done using a supercell of dimensions $15\times10\times10$ Å, and a cutoff energy of 1000 eV (requiring 64 000 plane waves per electron). Electronic structure calculations were performed at 20° and 10° intervals from 0° to 180° to map the potential and dipole curves. Each electronic structure calculation required approximately 60 T3D CPU hours, and where geometry optimization was included this increased sixfold. The 0° and 180° rotations correspond to the *cis* and *trans* conformations, respectively. The fixed geometry used to calculate the *nonoptimized curve* was chosen to be that of the fully relaxed 90° conformation. Figure 4(a) shows all the potential curves and the variations in the dipole moment with respect to conformation. The figure clearly shows that the *fully optimized* curve has significantly smaller barrier energies in relation to the *nonoptimized* curve. The differences in barrier heights are particularly large around 0°, where the effect of full optimization is to decrease the barrier by approximately 1.5 eV. Barrier heights are of importance in realistic molecular dynamics simulations of liquid crystals, as they take account of molecular flexibility. Both energy curves have two local minima, at approximately 60° and 120°, with the 60° minimum being the more stable. We return to this point below.

In order that the potential surface can be implemented in realistic empirical calculations, a parametrized function has been fitted to the torsional potential curve. The one-dimensional potential can be fitted by taking the important cosine terms in a Fourier series, thus

$$V(\Theta_r)=\sum_{n\in\{S\}} c_n\cos\left(\frac{2\pi n\Theta_r}{360}\right), \tag{2}$$

where $\{S\}$ is the set of indices to be summed over. The values of the coefficients, $c_n$, are given in Table II, and this curve is the one shown in Fig. 4(a) overlayed by the calculated points.

The conformation-dependent dipole moment magnitude for both curves is also shown in Fig. 4(a). It is apparent that the dipole is strongly influenced by conformation, but is otherwise relatively insensitive to molecular geometry. The dipole moments for the *fully optimized* curve and *nonoptimized* curve approximately converge at 50°, the same torsional angle at which the energy curves also converge. Investigation of the optimized geometries, calculated from the *fully optimized* curve, suggests this is due to relative changes in geometry between conformations. The largest changes in structure between conformations occur between 0° and 50°. This is due to the steric repulsion between the fluorine atoms which becomes insignificant when the torsional angle

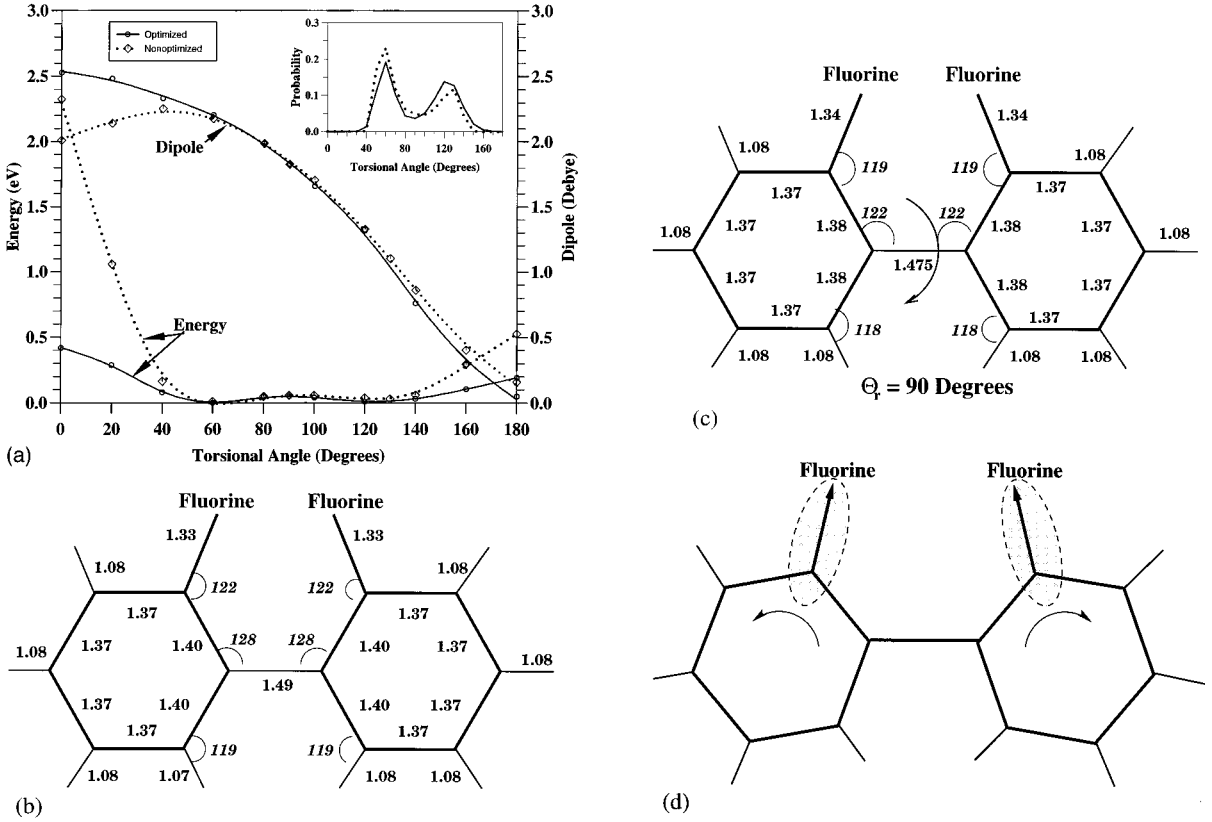


FIG. 4. (a) shows the torsional potential curve for 2-2' difluorobiphenyl as determined using both full molecular geometry optimization for each conformer and fixed molecular bond lengths and angles as described in the text. Calculations were performed at each 20° interval from 0° (cis) to 180° (trans). The molecular dipole as a function of torsional angle is also shown on the same plot. The curves (inset) show the relative probabilities of the conformations and the clear preference of the 60° to the 120° minimum at 300 K. (b) is a schematic illustration of the optimized molecular geometry in the planar conformation, and (c) shows the optimized 90° conformation for comparison. The distances are in Å, and both figures are projected onto a planar conformation for clarity. (d) shows a schematic diagram indicating the nature of bond deformation that occurs in the planar geometry. The highlighted areas indicate the dipolar regions.

is greater than 50°. The larger fluorine atoms have a significant influence on the geometry of the molecule, particularly in the planar conformation when the two fluorine atoms are adjacent to each other. Figures 4(b) and 4(c) give a comparison of two optimized structures in the 0° and 90° conformations. In the region 0°–50°, where electron overlap between the two fluorine atoms occur, the central bond bends such as to push the fluorines further apart. This effect is shown schematically in Fig. 4(d). Also shown in this figure are the two dipolar regions of the molecule which are located on the C-F bonds. These two areas of charge are the dipole components which are responsible for the overall molecular dipole. Both components are directed from the C to the F atoms, as shown in the figure. The total molecular dipole is the vector sum of the two dipoles, and hence is located at their center.

TABLE II. Coefficients of the fully optimized curve shown in Fig. 4(a) as described in the text. For a reasonable fit it is not necessary to use all coefficients.

| $n$ | $c_n$ | $n$ | $c_n$ |
|---|---|---|---|
| 0 | 0.009 859 | 5 | 0.007 895 |
| 1 | 0.069 780 | 6 | 0.001 767 |
| 2 | 0.117 665 | 7 | -0.006 103 |
| 3 | 0.041 277 | 8 | 0.001 506 |
| 4 | 0.070 496 | | |

The dipole vector is found to be predominantly in the $y$ and $z$ directions, moving in a path which follows the relative positions of the fluorine atoms. That is, it points in a direction which lies at half of the torsional angle between the two phenyl rings. A diagram showing the direction and magnitude of the molecular dipole as a function of torsional angle is given in Fig. 5.

A more physical insight into the plot of total energy against torsional angle, $\Theta_r$, for 2-2' difluorobiphenyl can be gained by recasting the energy scale as a probability density. This is done first by calculating the statistical partition function [29]

$$Z=\int d\Theta_r e^{-E(\Theta_r)/k_BT}, \tag{3}$$

which is the normalization constant for the probability density given by

$$P(\Theta_r)=\frac{e^{-E(\Theta_r)/k_BT}}{Z}, \tag{4}$$

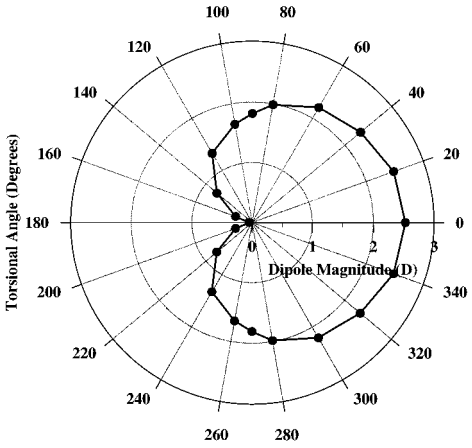


FIG. 5. Polar plot of molecular dipole for 2-2' difluorobiphenyl as viewed along the long molecular axis. The torsional angle $\Theta_r$ is related to the direction of the dipole $\Theta_D$ by $\Theta_D = \Theta_r/2$.

where $k_B$ is the Boltzmann constant, and $T$ is the given temperature, 300 K in this case. A plot of the probability is shown in Fig. 4(a) (inset) for both the *fully optimized* and *nonoptimized* potentials.

The probability curve for the *fully optimized* calculations shows the relative probabilities of the two minima which occur at 60° and 120°. Note that the *fully optimized* probability curve has the 120° conformation more highly populated than the *nonoptimized* curve, where the probability maximum is located at 128°.

The average dipole can be found by multiplying the probability density for a given temperature and the corresponding dipole magnitudes. This will give the molecular dipole moment as a function of temperature, as shown in Fig. 6. It can be seen that the dipole of the molecule decreases with temperature from 2.21 to 1.66 D at room temperature (300 K). This can be understood by examining the probability distribution with respect to temperature. The local energy minimum conformation at 120° becomes increasingly occupied as temperature rises, but this conformation has a lower dipole moment. The statistical weighting for this state becomes larger, and therefore the total averaged dipole decreases.

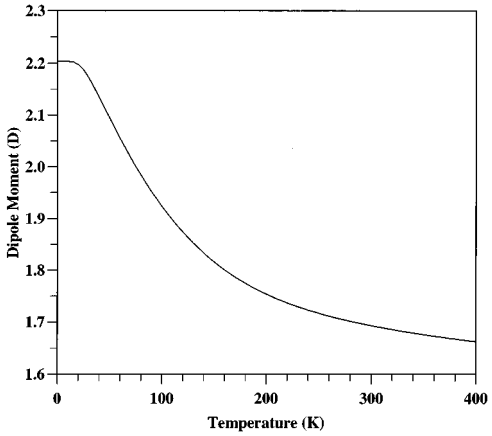


FIG. 6. Plot of the temperature dependence of the molecular dipole of 2-2' difluorobiphenyl as found from the Boltzmann-weighting scheme described in the text.

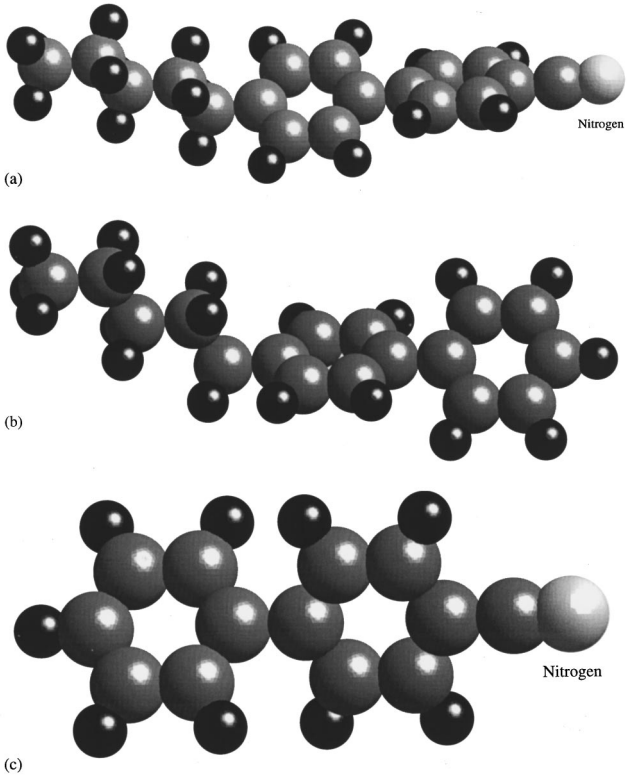


FIG. 7. Illustration of (a) the liquid crystal 5CB, (b) pentyl biphenyl (5B), and (c) cyano biphenyl (0CB) all in their respective minimium energy conformations.

### *3. 5CB and related fragments*

For a mesophase to form it is generally found that the terminal groups of the molecules contain permanent moments. However, the polarity of these groups frequently gives rise to very strong intermolecular attractions which raise the melting point of the compound [2]. Hence a thorough understanding of the origin of the polarity at a molecular level is of obvious importance. 5CB is one of the most well-characterized nematogens. It is composed of two phenyl rings (biphenyl) terminated by a CN (cyano) group at one end, and by a five-membered alkyl chain (pentyl) at the other. An illustration is shown in Fig. 7(a). It is generally recognized that the highly polar cyano group in 5CB accounts for most of its polarity, with the alkyl chain increasing the dipole through electron donation.

To quantify the effect of the terminal groups, we calculated dipoles for cyanobiphenyl (0CB as it contains no tail), 5CB and 4-4' pentyl biphenyl (5B, as it contains no cyano group). The minimum energy conformation of 5CB has a dihedral rotation angle of 31° [13], and an all-*trans* tail perpendicular to the adjoining phenyl group. For completeness the dipole of 5B and 0CB were calculated in the relative conformations that match the minimum conformation of 5CB. However, it was found that the dipole moment for 0CB and 5B (with an all-*trans* tail) shows no appreciable conformational dependence. This is in accord with previous work [13], which showed that the structures of these individual molecules do not change significantly with conformation. The results are shown in Table III.

The largest contribution to the dipole moment of 5CB comes from the cyano group since 0CB has a relatively large

TABLE III. Dipole moment magnitudes and directions for liquid crystal fragments and/or molecules as described in the text.

| Molecule | Conformation | Dipole moment $D$ | Vector direction |
|---|---|---|---|
| Phenyl benzoate | 0° | 2.07 | along C=O bond |
| Phenyl benzoate | 50° | 2.45 | along C=O bond |
| 0CB | 31° | 5.83 | tail to cyano group |
| 5B | 31° | 0.55 | tail to phenyl groups |
| 5CB | 31° | 6.50 | tail to cyano group |

dipole of 5.83 D. However the effect of the electron donating tail is evident as the dipole moment of 5B is 0.55 D. The addition of these fragment dipoles is 6.38 D, which is marginally smaller than the dipole of 5CB (6.50D). The results suggest that intramolecular charge transfer is not appreciable. This implies that simple vector addition of dipole moments of fragments provides a good estimate of the total molecular dipole.

## IV. SUMMARY AND CONCLUSIONS

In this paper we have explored the conformation-dependent molecular dipole moments for liquid crystal molecules and mesogenic fragments containing atoms of disparate electronegativity. The only approximations which enter our treatment are the well-established pseudopotential approximation for the valence electron – ion interaction, and the generalized gradient approximation for exchange and correlation. Since periodic boundary conditions are enforced and the molecular electronic wave function is expanded in a Fourier series (i.e., in plane waves), there is no bias toward any particular molecular bonding configuration. The results of our calculations are in reasonable agreement with available data both for conformational energy barriers and molecular dipole moments, and may serve to assist the experimental analysis where there is uncertainty.

We have tracked the molecular dipole in phenyl benzoate at two conformations, and conclude that the dipole is determined by the C=O double bond, and that it exhibits only a relatively weak but discernible dependence on conformation. This is in contrast to the case of fluorinated biphenyl for which the molecular shape (defined by the torsional angle) exerts a profound influence on the molecular dipole ranging from nearly zero to 2.5 D. The temperature dependence of conformer populations is found to give rise to an associated temperature dependence of the molecular dipole. In this particular case we observe a decrease of approximately 25% in the temperature range 0–300 K. In the case of the prototypical nematogen 5CB, we demonstrated that the vector sum of the dipole moments due to the isolated fragments is representative of the total molecular dipole moment. One of the principal advantages of our approach is that it relies on no empirical information or experimental input and can therefore be applied to molecular systems which are not yet synthesized, with no loss of accuracy.

## ACKNOWLEDGMENTS

We are grateful to the Edinburgh Parallel Computing Centre for access to the T3D Parallel supercomputer and to the UKCP grand challenge. We are also grateful to Cliff Jones of the Defence Research Agency, Mark Wilson of Durham University, and D. J. Cleaver of Sheffield Hallam University, for helpful discussions. C.J.A. and S.J.C. acknowledge the EPSRC. J.C. wishes to thank the Royal Society of Edinburgh and the Royal Society of London for support.

[1] E. B. Priestly *et al.*, *Introduction to Liquid Crystals* (Plenum, New York, 1975).
[2] L. M. Blinov, *Electrooptic Effects In Liquid Crystals* (Springer-Verlag, Berlin, 1994).
[3] M. G. Clark, K. J. Harrison, and E. P. Raynes, Phys. Technol. **11**, 232 (1980).
[4] F. Hardouin, A. M. Levelut, M. F. Achard, and J. Sigaud, J. Chim. Phys. **80**, 53 (1981).
[5] K. Satoh, M. Shigeru, and K. Shoichi, Liq. Cryst. **20**, 757 (1996).
[6] C. Zannoni (private communcation).
[7] D. Levesque, J. J. Weis, and G. J. Zarragoicoechea, Phys. Rev. E **47**, 496 (1993).
[8] H. Kresse, S. Tschierske, A. Hohmuth, C. Stutzer, and W. Weissflog, Liq. Cryst. **20**, 715 (1996).
[9] C. Jones, Ph.D. thesis, University of Hull, 1991.
[10] P. J. Wheately, *The Determination of Molecular Structure* (Dover, New York, 1968).
[11] S. J. Clark, C. J. Adam, G. J. Ackland, J. White, and J. Crain, Liq. Cryst. **22**, 469 (1997).
[12] S. M. Kelly, Liq. Cryst. **20**, 493 (1996).
[13] S. J. Clark, C. J. Adam, D. J. Cleaver, and J. Crain, Liq. Cryst. **22**, 477 (1997).
[14] L. J. Clarke, I. Stich, and M. C. Payne, Comput. Phys. Commun. **72**, 14 (1992).
[15] J. A. White and D. M. Bird, Phys. Rev. B **50**, 4954 (1994).
[16] L. Kleinman and D. M. Bylander, Phys. Rev. Lett. **48**, 1425 (1982).
[17] J. P. Perdew, J. A. Chevary, S. H. Vosko, K. A. Jackson, M. R. Pederson, D. J. Singh, and C. Fiolhais, Phys. Rev. B **46**, 6671 (1992).
[18] M. C. Payne, M. P. Teter, D. C. Allan, T. A. Arias, and J. D. Joannopoulos, Rev. Mod. Phys. **64**, 1045 (1992).
[19] M. Schluter and L. J. Sham, Phys. Today **35** (2), 36 (1982).
[20] J. S. Lin, A. Qteish, M. C. Payne, and V. Heine, Phys. Rev. B **47**, 4174 (1993).
[21] CERIUS 2.0 is a molecular modeling package distributed by Biosym Molecular Simulations Inc.
[22] A. Garcia, E. M. Cruz, C. Sarasola and J. M. Ugalde, J. Mol. Struct. Theochem. **363**, 279 (1996).
[23] A. J. Seed, K. J. Toyne, J. W. Goodby, and D. G. Mcdonnell, J. Mater. Chem. **5**, 1 (1995).

[24] J. W. Emsley, M. I. C. Furby, and G. Deluca, Liq. Cryst. **21**, 877 (1996).
[25] J. Crain, G. J. Ackland, and S. J. Clark, Rep. Prog. Phys. **58**, 705 (1995).
[26] H. Korner, A. Shiota, T. J. Bunning, and C. K. Ober, Science **272**, 252 (1996).
[27] M. Bremer, Adv. Mater. **7**, 867 (1995).
[28] H. Y. Yin and J. X. Wen, Liq. Cryst. **21**, 217 (1996).
[29] F. Mandel, *Statistical Physics* (Wiley, New York, 1988).